The EMBO Journal (2007) 26, 1–8 | © 2007 European Molecular Biology Organization | All Rights Reserved 0261-4189/07
www.embojournal.org

THE EMBO JOURNAL

Membrane potential governs lateral segregation of plasma membrane proteins and lipids in yeast

Guido Grossmann[1,4], Miroslava Opekarová[2,4], Jan Malinsky[3,4], Ina Weig-Meckl[1] and Widmar Tanner[1,*]

[1]University of Regensburg, Cell Biology and Plant Physiology, Regensburg, Germany, [2]Institute of Microbiology, Academy of Sciences of the Czech Republic, Videnska, Czech Republic and [3]Institute of Experimental Medicine, Academy of Sciences of the Czech Republic, Videnska, Czech Republic

The plasma membrane potential is mainly considered as the driving force for ion and nutrient translocation. Using the yeast *Saccharomyces cerevisiae* as a model organism, we have discovered a novel role of the membrane potential in the organization of the plasma membrane. Within the yeast plasma membrane, two non-overlapping subcompartments can be visualized. The first one, represented by a network-like structure, is occupied by the proton ATPase, Pma1, and the second one, forming 300-nm patches, houses a number of proton symporters (Can1, Fur4, Tat2 and HUP1) and Sur7, a component of the recently described eisosomes. Evidence is presented that sterols, the main lipid constituent of the plasma membrane, also accumulate within the patchy compartment. It is documented that this compartmentation is highly dependent on the energization of the membrane. Plasma membrane depolarization causes reversible dispersion of the H^+-symporters, not however of the Sur7 protein. Mitochondrial mutants, affected in plasma membrane energization, show a significantly lower degree of membrane protein segregation. In accordance with these observations, depolarized membranes also considerably change their physical properties (detergent sensitivity).

The EMBO Journal (2007) **26,** 1–8. doi:10.1038/sj.emboj.7601466; Published online 14 December 2006
Subject Categories: membranes & transport
Keywords: H^+-symporters; lipid rafts; membrane compartmentation; susceptibility against detergents

Introduction

Biological membranes were long considered to be a fluid mixture of lipids organized in a homogenous bilayer, which serves as a solvent for membrane proteins. In contrast, current models accent the high lateral compartmentation of membranes, consisting of distinct domains housing specific lipids and proteins. At the present time, the field is dominated, although not unchallenged, by the so-called 'lipid raft' concept (Simons and Ikonen, 1997; Brown and London, 1998; Anderson and Jacobson, 2002; Heerklotz, 2002; Edidin, 2003; Munro, 2003; Kusumi *et al*, 2004; Lagerholm *et al*, 2005), according to which sphingolipids with long acyl chains associate with sterols forming microdomains (rafts) within the membrane. This spontaneous separation of membrane lipids generates different environments for proteins within the membrane. An alternative mechanism of raft formation *in vivo* could rely on protein/protein interactions as the primary determinant of imminent specific lipid environment of individual types of proteins. Concerning the functions, it is postulated that proteins present in lipid rafts play a major role in processes like intracellular trafficking and signaling (Brown and London, 1998; Galbiati *et al*, 2001).

In *Saccharomyces cerevisiae*, two different non-overlapping lateral plasma membrane compartments have so far been distinguished. The membrane compartment occupied by Pma1p that we call MCP (this neutral designation is preferred to the previously used RMC P and RMC C for raft-based membrane compartment P and C; (Malinska *et al*, 2004)) and the other compartment accommodating arginine/H^+-symporter Can1p (Malinska *et al*, 2003), uracil/H^+-symporter Fur4p and Sur7p, a protein presumably involved in endocytosis, named MCC (this neutral designation is preferred to the previously used RMC P and RMC C for raft-based membrane compartment P and C; Malinska *et al*, 2004) (according to Can1p; Malinska *et al*, 2004). The lipid composition and functional relevance of these membrane compartments is unclear. A putative role in endocytosis has recently been suggested for eisosomes, cytosolic structures comprising one plasma membrane protein, Sur7p, (Walther *et al*, 2006), localized into MCC by our group.

In the resolution of fluorescence microscopy, MCC and MCP together cover the whole plasma membrane surface. However, in contrast to mammalian cells, yeast membrane domains are sufficiently large and distant from each other to be resolved. Whereas MCC consists of isolated patches about 300 nm in diameter, MCP exhibits a complementary, network-like pattern. Yeast plasma membrane is partitioned into two discernible plasma membrane compartments, and represents therefore a unique system for direct observation of the *in vivo* dynamics of membrane compartmentation. MCC- and MCP-specific markers in this genetically well-defined model organism can be used to monitor individual membrane domains, as they respond to changes in cell physiology. This should allow us to investigate processes involved in lateral segregation of membrane components.

The distribution of the MCC patches in the plasma membrane is strikingly stable. The patches do not change their relative positions within a time interval comparable to the yeast cell division cycle (Malinska *et al*, 2003). The pattern remains stable even after depolymerization of the actin or

*Corresponding author. Cell Biology and Plant Physiology, University of Regensburg, 93040 Regensburg, Germany.
Tel.: +49 941 943 3018; Fax: +49 941 943 3352;
E-mail: sekretariat.tanner@biologie.uni-regensburg.de
[4]These authors contributed equally to this work

Received: 28 June 2006; accepted: 24 October 2006; published online: 14 December 2006

tubulin cytoskeleton (Malinska *et al*, 2004). We now report that some MCC-specific proteins are released from the patches after the plasma membrane is depolarized.

In this study, in addition to inherent yeast plasma membrane proteins, we use a heterologously expressed hexose uptake protein HUP1, a glucose/H^+-symporter of *Chlorella kessleri* (Sauer *et al*, 1990). This protein proved to be an excellent model of an MCC protein, as its GFP fusion is functionally expressed in yeast and it accumulates in MCC (Grossmann *et al*, 2006). HUP1-GFP is exclusively and efficiently routed to the yeast plasma membrane and remains there for days; it is obviously not recognized by the yeast endocytic and membrane protein turnover systems. With HUP1-GFP, we demonstrate that the distribution of the plasma membrane components changes in response to changes in the membrane potential. Partial depolarization of the plasma membrane caused by HUP1-mediated proton uptake, an uncoupler, by mitochondrial mutations, or by applying an external electric field, results in a massive redistribution of HUP1-GFP molecules. Depending on the treatment, HUP1 can distribute even homogeneously in the plasma membrane after depolarization. Yeast H^+-symporters Can1p and Fur4p, and also the tryptophan permease Tat2p, a newly identified member of MCC, also move out of the patches under depolarizing conditions. On the other hand, the Pma1p and Sur7p distributions are not affected. When the membrane potential is restored, the proteins move back to the MCC patches re-constituted at their original positions.

We show that sterols are enriched in MCC and, hence, ergosterol colocalizes with the H^+-symporters and Sur7p in the plasma membrane. Our data indicate that on membrane depolarization, ergosterol, together with the H^+-symporters, moves out of the MCC patches. Moreover, not only the distribution of its components, but also the general properties of the plasma membrane are affected by the changes in the membrane potential. For instance, we document that the depolarized membrane is less susceptible to detergents.

Results

Ergosterol is accumulated within the membrane compartment C

Exponentially growing *S. cerevisiae* cells were stained with filipin, the fluorescent anti-fungal compound that interacts with 3′-β-hydroxy sterols (Norman *et al*, 1972). The plasma membrane was not stained homogeneously, rather in distinct patches (Figure 1A). The pattern is reminiscent of the appearance of Sur7- and Can1-GFP described previously, which were shown to colocalize in MCC (Young *et al*, 2002; Malinska *et al*, 2003, 2004). Figure 1C and D (see merge and fluorescence intensity profiles) show the almost perfect colocalization of filipin fluorescence with the fluorescence of Sur7-GFP. Walther *et al* (2006) documented that Sur7p colocalizes with two cytoplasmic proteins Pil1 and Lsp1 in assemblies termed 'eisosomes'. The deletion of Pil1p resulted in a redistribution of Sur7p from the patches (Walther *et al*, 2006). As we showed that Sur7p occupies MCC together with filipin-stained sterols and H^+-symporters, we checked whether the same deletion affects the membrane pattern of these membrane components. In fact, in *pil1*Δ cells, filipin-

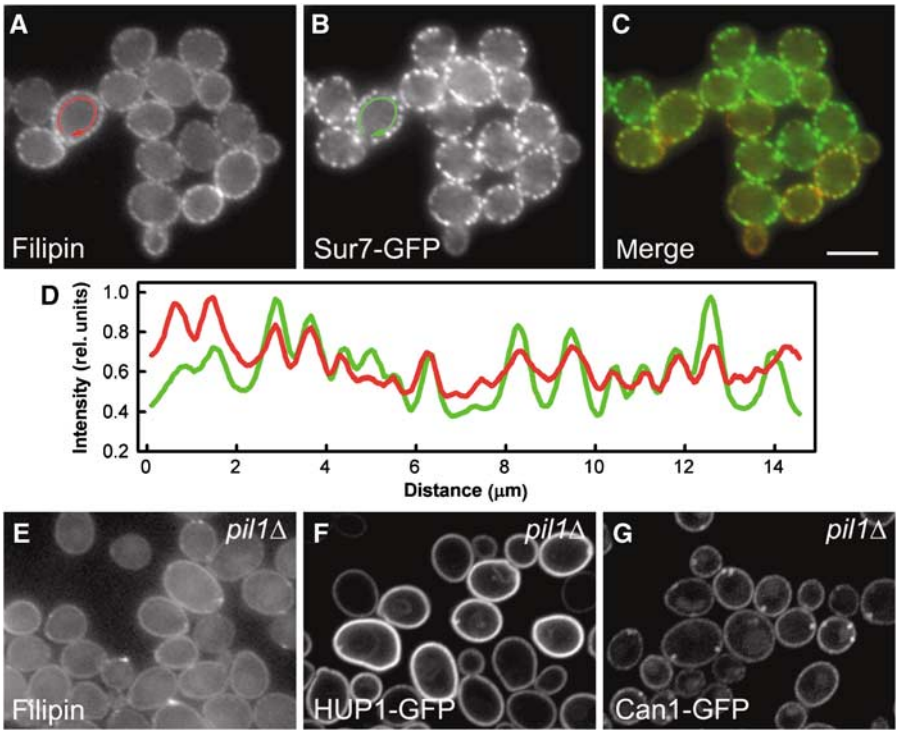

Figure 1 Sites of sterol accumulation in plasma membrane colocalize with MCC. Simultaneous localization of filipin-stained sterols (A; red in C, D) and an MCC marker Sur7GFP (B**;** green in C, D) was performed in living GYS48 cells. Wide-field fluorescence micrographs (**A–C**) and the fluorescence intensity profiles along the cell surface (**D**; outside the arrows in A, B) are presented. The curves in (D) were smoothed using a mean filter to reduce the noise and normalized to the same maximum value. Distribution of filipin-stained sterols in *pil1*Δ mutant (GYS130; **E**) was compared with HUP1 (**F**) and Can1p (**G**) patterns in these cells (strains GYS131 and GYS132, respectively). Again, wide-field image is presented in (E), whereas confocal sections are shown in (F, G). Bar: 5 μm.

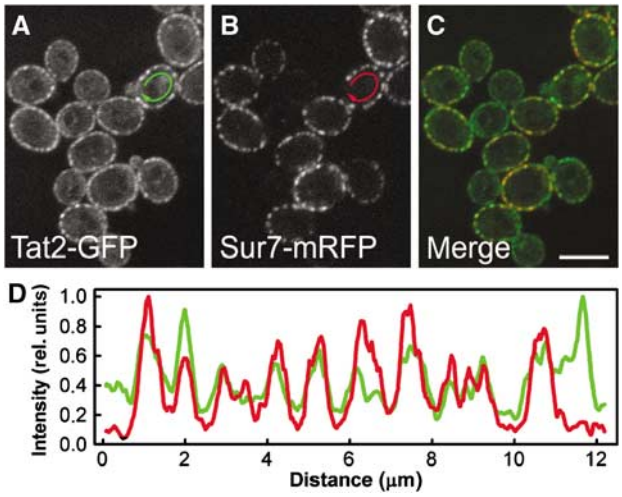

Figure 2 Tat2p is a part of MCC. Simultaneous localization of the tryptophan permease Tat2GFP (**A;** green in **C**) and the MCC marker Sur7mRFP (**B;** red in C) was performed in living GYS122 cells. Fluorescence intensity profiles along the cell surface (**D**; outside the arrows in A, B; green: Tat2GFP; red: Sur7mRFP) are presented. The curves in (D) were smoothed using a mean filter to reduce the noise and normalized to the same maximum value. Bar: 5 μm.

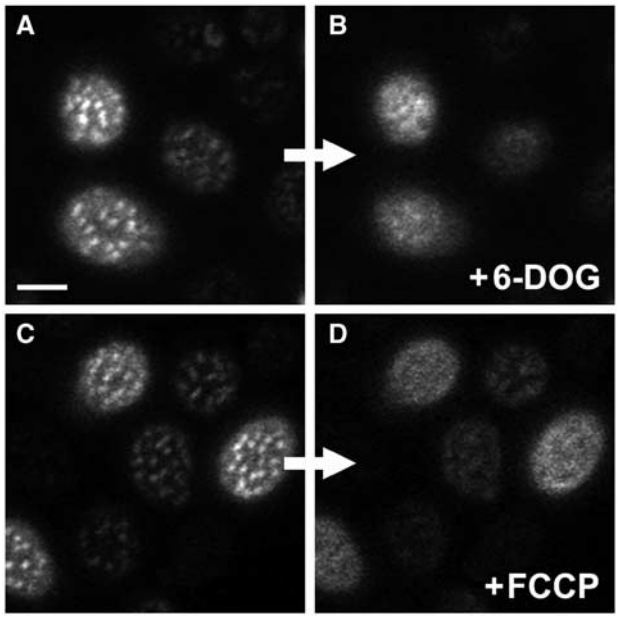

Figure 3 HUP1 patches are dissolved after plasma membrane depolarization. Changes in the distribution of HUP1GFP in the plasma membrane of living cells depolarized by 6-DOG uptake (strain GYS118; **A, B**) or FCCP treatment (strain GYS110; **C, D**; see Materials and methods for details) were observed. Surface confocal sections of the same cells before (A, C) and after the treatment (B, D) are presented. In both cases, the protein was released from MCC patches after plasma membrane depolarization. Only remnants of patches are visible in some treated cells. Bar: 2 μm. For corresponding time-lapse observations, see Supplementary Movies S1–3.

stained sterols and MCC markers Can1p and HUP1 distributed homogenously within the plasma membrane, with occasional accumulations in a few bright clusters (Figure 1E–G), as was reported for Sur7p (Walther *et al*, 2006).

Ergosterol is required for plasma membrane targeting of the high-affinity tryptophan/H^+-symporter Tat2p (Umebayashi and Nakano, 2003). We therefore tested whether filipin-stained sterols and Tat2-GFP colocalize in the plasma membrane. Using the MCC marker Sur7-mRFP, a complete overlap of the fluorescence signals was detected (Figure 2A–D). Consequently, we conclude that ergosterol, together with Tat2p, is part of MCC.

The membrane potential affects the composition of MCC

An *hxt1-7*Δ yeast strain (RE700), which is unable to grow on glucose as the sole carbon source, is rescued when transformed with *C. kessleri* hexose/H^+-symporter HUP1 (Robl *et al*, 2000). Heterologous HUP1 accumulates in the yeast MCC (Grossmann *et al*, 2006). Addition of glucose to *hxt1-7*Δ cells expressing HUP1-GFP causes changes in the patchy distribution of the fluorescent protein; the patchy pattern disappeared to a significant degree within a few minutes (not shown). The same effect was induced by the addition of the non-metabolized glucose analogue, 6-deoxy-D-glucose (6-DOG), which is also a substrate for HUP1 (Figure 3A and B; see also Supplementary Movies S1 and S2). This suggested that the observed effect did not result from the subsequent metabolism of the transported sugar, rather from the transport process itself. Addition of substrates to H^+-symporting systems causes transient depolarization of the plasma membrane (for HUP1, see Komor and Tanner, 1976). We therefore hypothesized that the localization of HUP1-GFP in the patches depends on the membrane potential.

To test this hypothesis, the cells expressing HUP1-GFP (strain GYS110) were treated with the proton gradient uncoupler, FCCP (carbonyl cyanide 4-(trifluoromethoxy)phenylhydrazone), or with inhibitors of ATP synthesis, sulfite or azide. After the FCCP treatment, the patchy pattern of HUP1-GFP disappeared in less than 1 min, and the fluorescence became almost homogenous (Figure 3C and D; see also Supplementary Movie S3). Inhibitors of ATP synthesis had the same effect; however, it took longer until the protein redistribution was evident (not shown). As it turned out to be difficult to remove the inhibitors sufficiently to test the reversibility of the phenomenon, we attempted to achieve membrane depolarization by a pulse of an external electric field, as is generally used for electroporation (transient membrane pore formation). Applying a current of 15 mA between two platinum electrodes 1 cm apart to immobilized cells for 1 min caused HUP1-GFP release from the patches. After 10–20 min of recovery, the HUP1-GFP patches re-formed in their original positions (Figure 4).

We also tested whether the endogenous protein components of MCC show the same dependence on the membrane potential. Can1-GFP patches also dispersed when FCCP was added (Figure 5A). The process, however, took about twice as long as compared to the time required for spreading of HUP1-GFP. Apparently, the release of Can1-GFP from the MCC patches was also caused by membrane depolarization: when the external pH was increased to 7.0 to prevent net proton influx, the Can1-GFP distribution remained unchanged after FCCP treatment (Figure 5B). Fur4-GFP (KM162) and Tat2-GFP (GYS121) behaved essentially as Can1-GFP (not shown). In contrast, Sur7-GFP was not released from the patches after FCCP treatment (Figure 5C). The same was true for the complementary fluorescence

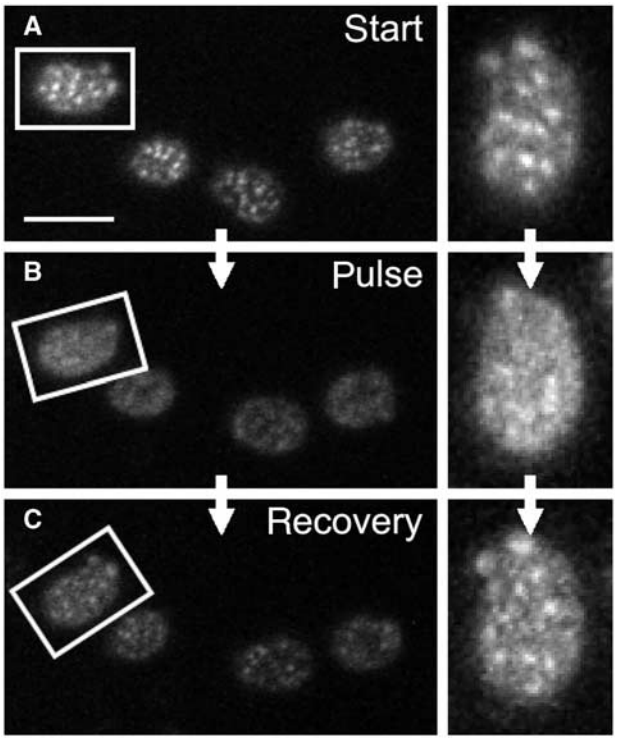

Figure 4 Depolarization-induced changes in HUP1 distribution are reversible. For membrane depolarization, 1 min pulse of external electric field was applied on exponentially growing cells expressing HUP1GFP (strain GYS110) in order to depolarize the plasma membrane. The distribution of the protein before (**A**), immediately after (**B**) and 20 min after depolarization (**C**) is shown. Aligned surface sections of one cell are also presented (right). Despite the increased signal-to-noise ratio caused by phototobleaching of HUP1GFP fluorescence during the scanning, the restored pattern of MCC patches almost identical to that in (A) is clearly visible in (C). Bar: 5 μm.

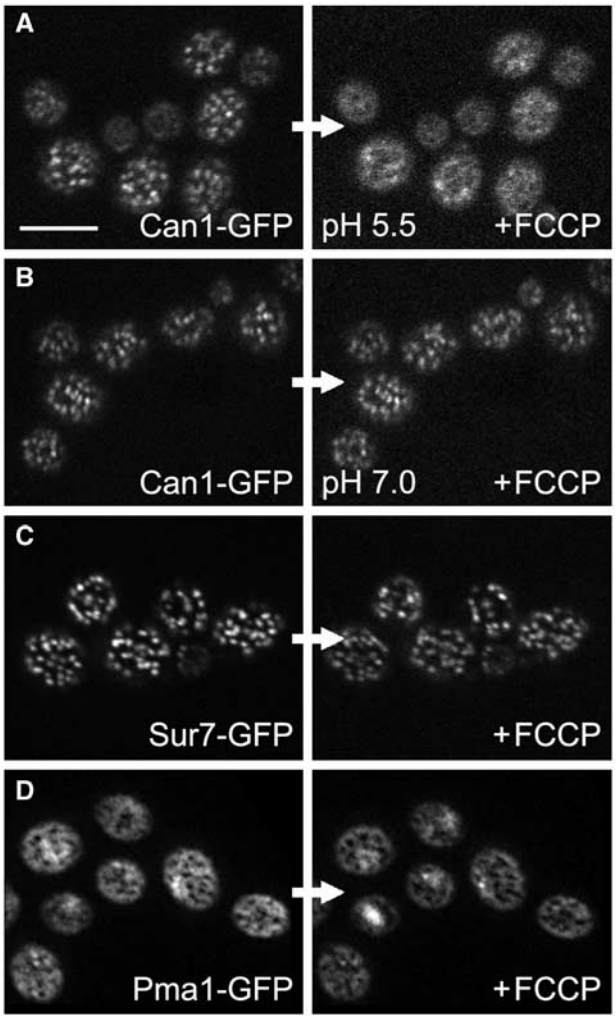

Figure 5 Only some MCC proteins are affected by plasma membrane depolarization. The plasma membrane of living cells expressing Can1GFP (**A, B**), Sur7GFP (**C**) and Pma1GFP (**D**) (strains GYS113, GYS48 and KM12, respectively) was depolarized by FCCP. Surface optical sections of cells before (left) and after depolarization (right) are shown. Only Can1GFP pattern (A) was dissolved after the treatment. Neither Sur7GFP nor Pma1GFP plasma membrane distribution was affected (C, D). When the depolarization effect of FCCP was prevented using buffer of pH 7.0 during the treatment, no release of Can1p from MCC patches was observed (B). Bar: 5 μm.

pattern of Pma1-GFP residing in MCP. Pma1p did not penetrate MCC after membrane depolarization (Figure 5D).

The plasma membrane distribution of HUP1-GFP was analyzed in respiration-deficient mutants *atp1*Δ and *cox7*Δ. The null mutant *atp1*Δ lacks the alpha subunit of the mitochondrial F1F0 ATP synthase, whereas in *cox7*Δ, the gene for the cytochrome *c* oxidase subunit VII is deleted. Both mutant strains are unable to grow on respiratory carbon sources (Takeda *et al*, 1986; Aggeler and Capaldi, 1990; Steinmetz *et al*, 2002). The defective energy metabolism results in a decrease of the plasma membrane ATPase activity, and therefore, in a reduced membrane potential. Compared to the wild type, both respiratory-deficient strains exhibit a significantly more dispersed localization of HUP1-GFP. Figure 6 shows the HUP1-GFP surface pattern in the mutants *atp1*Δ and *cox7*Δ, as well as a decreased uptake of ^{3}H-tetraphenylphosphonium bromide (^{3}H-TPP^{+}), a probe for monitoring the magnitude of the membrane potential (Komor and Tanner, 1976; Vallejo and Serrano, 1989).

The behavior of ergosterol patches in depolarized membranes was not easy to follow. When the FCCP was added to filipin-stained cells, the filipin pattern remained unchanged. Moreover, even the release of the H^{+}-symporters from the MCC patches was hindered in these cells (Figure 7). In this case, the stabilization of the MCC patches can be attributed to the formation of quite stable stoichiometric complexes of filipin with sterols (Norman *et al*, 1972; Kruijff and Demel, 1974). This suggests that, not only Tat2p, but also other H^{+}-symporters accumulated in MCC require an ergosterol-rich lipid environment. When the cells were treated in the opposite order, first depolarized by FCCP and then stained by filipin, the intensity of the filipin fluorescence was significantly lower, and no accumulation of filipin-stained sterols in MCC patches could be detected anymore (not shown). It is most unlikely that this reflects a loss of sterols from the membrane within seconds, rather a dilution of ergosterol concentration in the patches, once the sterol is spread within the whole membrane. According to the deduced interaction, formation of large stoichiometric complexes of sterols with polyenes (Kruijff and Demel, 1974), a reduced local sterol concentration would be expected to severely affect the efficiency of filipin staining.

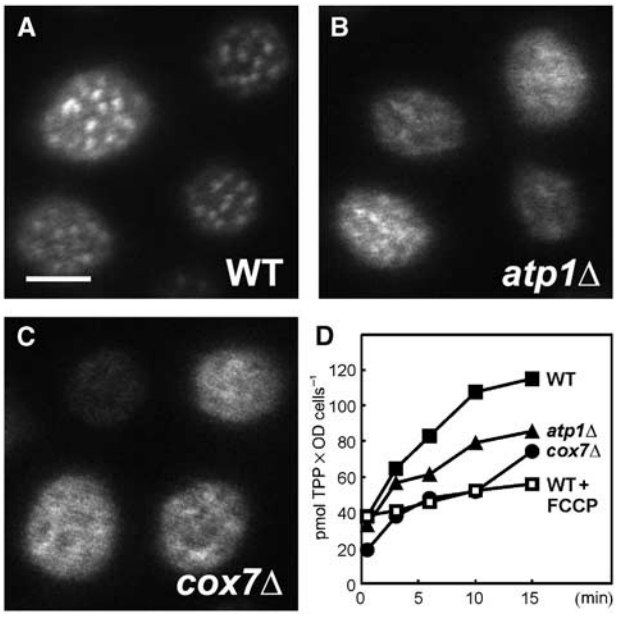

Figure 6 The distribution of HUP1GFP is impaired in mutants deficient in mitochondrial respiration. Surface scans of WT cells (**A**), *atp1*Δ and *cox7*Δ mutants (**B, C**), all expressing HUP1GFP. For *atp1*Δ and *cox7*Δ, a considerably lowered membrane potential was detected by measurement of the uptake of ^{3}H-TPP as compared to untreated and FCCP-treated WT cells (**D**). Bar: 2 μm.

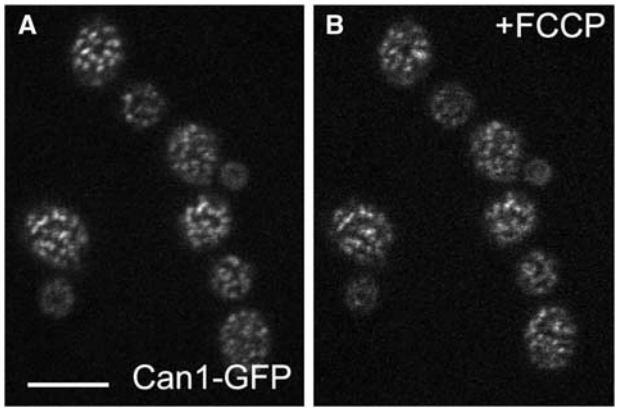

Figure 7 Filipin stain prevents the release of Can1p from MCC. Cells expressing Can1GFP (strain GYS113) were stained by filipin and observed under agarose. These cells show the characteristic MCC pattern of Can1GFP fluorescence (**A**). To the same cells immobilized in agarose, 50 μM FCCP was added. The Can1-GFP pattern does not change (**B**) (compare with Can1-GFP cells depolarized by FCCP without filipin treatment; Figure 5A, right). Bar: 5 μm.

The depolarized plasma membrane is less sensitive to detergents

Massive reorganization of the membrane components after membrane depolarization, as documented above, is likely to be accompanied by a change in the membrane properties. Previously, we observed (Komor *et al*, 1979) that various cells (*S. cerevisiae*, *C. kessleri*, *Escherichia coli*) were less sensitive to a number of detergents when these cells were treated with inhibitors of energy metabolism before the detergent was added. In the light of our findings, the phenomenon could be related to the membrane depolarization-induced changes in the plasma membrane structure. In Figure 8, we demonstrate

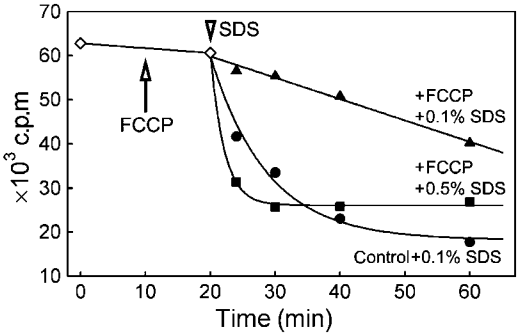

Figure 8 Leakage of AIB from the cells with depolarized plasma membrane. Cells accumulating radioactive AIB (strain BY4742) were treated with 0.1% SDS (arrowhead) in the absence (●) or presence of 20 μM FCCP (▲). The efflux of accumulated radioactivity was much slower in the presence of FCCP. Considerably higher detergent concentration (0.5% SDS; ■) was necessary to induce an effect comparable to that observed in FCCP-untreated cells. Note that the addition of FCCP at $t = 10$ min (arrow) had no effect on the membrane permeability for AIB (◇).

that yeast cells that have accumulated the radioactive amino-acid analogue α-amino-isobutyric acid (AIB) rapidly lose this compound after the addition of 0.1% SDS. This leakage is considerably diminished when the cells are uncoupled by FCCP before the detergent treatment. A five-fold higher concentration of SDS was required to achieve the same rate of AIB leakage from FCCP-treated cells, compared with the control. We conclude that the depolarized membrane is much less accessible for detergent molecules.

Discussion

All the proteins so far reported to segregate into lateral domains within the plasma membrane of *S. cerevisiae* are components of detergent-resistant membranes (DRM; Bagnat *et al*, 2000; Lee *et al*, 2002; Dupre and Haguenauer-Tsapis, 2003; Hearn *et al*, 2003; Malinska *et al*, 2003, 2004; Umebayashi and Nakano, 2003; Grossmann *et al*, 2006). If we accept the idea that DRMs reflect the existence of lipid rafts, at least two different types of rafts must be distinguished in the yeast plasma membrane: rafts containing Pma1p within MCP, and rafts containing Sur7p and various H^{+}-symporters in MCC. In fact, different lipid requirements were reported for proteins residing in either MCP or MCC. Gaigg *et al* (2005) showed that C_{26} acyl chains, but not ergosterol, are required for proper sorting of Pma1p. In the plasma membrane, Pma1p is, in fact, associated with sphingolipids (Lee *et al*, 2002). On the other hand, sterols were shown to be necessary for correct targeting of Tat2p (Umebayashi and Nakano, 2003), which we show to be accumulated in MCC (Figure 2A–D). These findings suggest that sphingolipid-rich and sterol-rich domains might exist and are in accordance with our observation that filipin-stained sterols accumulated in MCC patches (Figure 1). A three-fold enrichment of ergosterol in MCC can be estimated from the relative filipin intensities inside and outside the patches. As the area surrounding the patches of MCC corresponds to the MCP compartment (Malinska *et al*, 2003, 2004), the plasma membrane ATPase, Pma1p, is obviously located in an area low in ergosterol, supporting thus the data of Gaigg *et al* (2005). Although the interpretation of all the data above

seems fully conclusive, it is based in part on staining with filipin. Caution for potential toxic effects of filipin has to be taken into account. In addition, the possibility that after the addition of filipin, not the ergosterol but filipin–ergosterol complexes are visualized has to be considered.

The number and positions of the MCC patches were shown to be stable (Malinska *et al*, 2003) and independent of the main cytoskeletal components (Malinska *et al*, 2004). However, the expression of proteins like Can1p, Fur4p or Tat2p, and consequently their appearance in the plasma membrane, is substrate-regulated (Seron *et al*, 1999; Kodama *et al*, 2002). Therefore, these proteins appear in the patches in different amounts and at different times. Thus, the composition of the MCC patches changes in time and depends on the cell physiology.

In this study, we demonstrate the dynamics of the MCC composition from a different point of view. We show another factor that affects the composition of this compartment: the plasma membrane depolarization accompanying the actual transport causes the release of an H^+-symporter from its original patchy location. In Figure 3A and B, this is demonstrated for a heterologously expressed hexose transporter HUP1. Using two other independent approaches—selective proton gradient uncoupling by FCCP and membrane depolarization by an external electric field—we show that this redistribution of plasma membrane proteins is actually caused by membrane depolarization (see also Supplementary data).

In addition, experiments with mutants, affected in mitochondrial respiration, lead to the same conclusion. In these mutants, impaired ATP synthesis affects the plasma membrane H^+-ATPase and thus the plasma membrane potential. Using our marker protein HUP1-GFP, we were able to visualize the altered protein segregation within the plasma membrane of these mutants.

Several observations indicate that ergosterol, the main sterol component of yeast plasma membrane, also moves out from the MCC patches after membrane depolarization: (i) ergosterol is obligatorily needed for Tat2p trafficking. In the plasma membrane, Tat2p is always found associated with DRM-containing sterols (Umebayashi and Nakano, 2003). It is therefore legitimate to suppose that Tat2p and ergosterol also move together in the membrane; (ii) association of MCC proteins with (sterol-rich) DRM is not disturbed even in isolated membranes (floating gradients); the HUP1 protein expressed in yeast and purified to homogeneity contained still an amount of two molecules of ergosterol per molecule of protein (Robl *et al*, 2000); (iii) the release of Can1p from the MCC patches is hindered in the presence of filipin (Figure 7), which is known to form stable complexes with 3′-β-hydroxy sterols (Norman *et al*, 1972); (iv) H^+-symporters accumulated in MCC and filipin-stained sterols always show the same distribution: patchy pattern in the wild-type cells and homogeneous distribution in the plasma membrane of *pil1*Δ cells (Figure 1E–G).

Membrane reorganization in response to the membrane potential has already been observed. Schäffer and Thiele (2004) showed that membrane potential induces de-mixing into domains within membranes consisting of lipids having different lengths. Herman *et al* (2004) reported an increased phase transition temperature in a pure phospholipid bilayer, when a Nernstian potential, negative inside, was applied. This indicates that, in the presence of a potential, the membrane organizes in a more ordered state. The higher mobility of membrane compounds, characterized by a lower phase-transition temperature in the absence of a membrane potential, is in accordance with our observations that membrane proteins can move out of the MCC patches after membrane potential disruption. Lipid–protein interactions are not affected, as Tat2p and other proteins move together with their specific lipid environment. Hence, the only change in the structure of a depolarized membrane would be a shift in the equilibrium between the large ergosterol-rich patches and possibly small ergosterol-rich domains of the type found in animal cells, which are not distinguishable by fluorescence microscopy. This interpretation is supported by the observation that HUP1-GFP behaves identically towards the Triton X-100 extraction, independently of whether the cells are treated with FCCP or not, that is, whether the protein is localized in patches or is diffused within the plasma membrane (data not shown).

In this context, re-formation of HUP1-GFP patches after the cells recover from depolarization (Figure 4), is obvious. As is clear from Sur7p and Pma1p fluorescence (Figure 5C and D), the pattern of the MCC compartment does not change either in the number or in the distribution of the patches, although their composition is changed after depolarization: at least some H^+-symporters and ergosterol are released from the patches. After the membrane potential is re-established, the released MCC components return back to the patches (marked by Sur7p and most likely also by other proteins). While the stability of the Sur7p pattern can be attributed to its association with large immobile protein assemblies at the cell cortex (Roelants *et al*, 2002; Walther *et al*, 2006), the mechanism of the accumulation of H^+-symporters in the same compartment and their release in response to membrane depolarization is not really understood. It is interesting that up to now only H^+-symporters have been found to respond to the membrane potential and change their position. Potential-dependent conformational changes of these symporters, which could affect both protein–protein and/or protein–lipid interactions, may thus be involved in this dislocation.

Together with the distribution of the plasma membrane components, the general properties of the membrane are changed after depolarization. In Figure 8, we show that the plasma membrane of the depolarized cells is much less sensitive to SDS treatment. This is in accordance with the observations of Komor *et al* (1979), who found lowered susceptibility of uncoupled cells towards various detergents. At this stage, we can only offer two speculative explanations. One of these is related to the more disordered structure of the depolarized plasma membrane—the observed effect could reflect a lower accessibility of highly mobile membrane components for interaction with detergent molecules. The other explanation comprises a change in membrane packing related to the sterol relocalization, which could make the membrane proteins less accessible for detergents. A similar effect was reported some time ago, when it was shown that nystatin lost its inhibitory activity in de-energized cells (Komor *et al*, 1979; Malewicz and Borowski, 1979), and now in this study, where we observed strikingly low sterol staining by filipin after the FCCP treatment. This unlikely is due to a sudden loss of sterols from the membrane. As it has

been proposed that eight polyene molecules intercalate into a cluster of eight sterols (Kruijff and Demel, 1974), a dispersal of sterols within the total membrane surface leads to a situation that the local concentration of sterols becomes limiting for the staining reaction as well as for the harmful action of polyenes.

Finally, the functional importance of the compartmentation of transport proteins in the yeast plasma membrane should at least be briefly mentioned. Recently, we have described a significant decrease in glucose uptake via the HUP1-H^+-symporter in an *erg6*Δ mutant that shows a homogenous membrane distribution of HUP1-GFP (Grossmann *et al*, 2006). The general amino-acid transporter Gap1 was shown to be completely inactive, when mutants were defective in the synthesis of raft-forming lipids, and the protein did not partition into DRM fractions any more (Lauwers and André, 2006; Lauwers and André, personal communication). Both the examples point to the importance of the protein association with specific lipids not only for their trafficking but also for their activity *in situ*.

Materials and methods

Strains and growth conditions

Plasmid amplification was carried out in the *E. coli* host XL1-Blue (Bullock *et al*, 1987). The bacterial strains were grown at 37°C in 2TY medium (1% trypton, 1.6% yeast extract, 0.5% NaCl) supplemented with ampicillin (100 μg/ml) for selection of transformants. *S. cerevisiae* strains used in this study are listed in Supplementary Table SI (Reifenberger *et al*, 1995; Brachmann *et al*, 1998). Yeast cells were cultured in a rich medium (YPD; 2% peptone, 1% yeast extract, 2% glucose) or in a synthetic minimal medium (SD; 0.67% Difco yeast nitrogen base without amino acids, 2% glucose, supplemented with essential amino acids). Well-pronounced patchy pattern of HUP1-GFP was detected at low (0.2%) glucose concentration. Cells expressing *CAN1*, *FUR4* or *TAT2* were cultured as described (Malinska *et al*, 2003, 2004; Umebayashi and Nakano, 2003). In all experiments, early logarithmic cells were used.

Construction of plasmids

YIplac211GFP, *YIplac128GFP* and *YIplac128mRFP:* EGFP and mRFP genes, obtained by cutting pVT100U-GFP and pVT100U-mRFP (J Stolz, unpublished) with *Hin*dIII and *Mfe*I, were inserted into the integrative plasmids YIplac211 and YIplac128 containing selection markers *URA3* and *LEU2*, respectively (Gietz and Sugino, 1988), both cut with *Hin*dIII and *Eco*RI. *YIp211CAN1GFP:* CAN1 gene was inserted as an *Xho*I–*Xba*I fragment into YIplac211GFP tagging vector. Before transformation, the plasmid was linearized by digestion with *Bcu*I. *YIp211SUR7GFP* and *YIp211SUR7mRFP:* SUR7 gene was inserted as a *Hin*dIII–*Bam*HI fragment into YIplac211GFP and YIp211mRFP, respectively. The plasmids were linearized by *Eco*52I. *YIplac211TAT2GFP:* TAT2 gene was inserted as a *Hin*dIII–*Xho*I fragment into YIplac211GFP and linearized by *Eco*147I.

Filipin staining

Living cells were washed in 50 mM potassium phosphate buffer, pH 5.5, diluted to $A_{600} = 0.3$, stained with 5 μg/ml filipin (Sigma) for 5 min, washed again in the same buffer, concentrated by brief centrifugation and observed.

Microscopy and plasma membrane depolarization

Wide-field images were acquired using fluorescence microscope Axiovert 200 M with × 100 PlanApochromat objective (NA = 1.4), coupled to AxioCam HRc camera (Zeiss). Confocal sections were scanned by LSM510-Meta confocal microscope (Zeiss). Fluorescence signals of filipin (exc. 360–370 nm/em.; 397 nm long pass), GFP (wide field 450–490/515 nm long pass, confocal 488/505–550 nm) and mRFP (543/580–615 nm) were detected. In double labeling experiments, sequential scanning was used to avoid any crosstalk of fluorescence channels. Living cells were washed in 50 mM potassium phosphate buffer (pH 5.5), immobilized by thin film (~0.5 mm) of 1% agarose (23°C) and observed. Substances added during observation (6-DOG, FCCP; final concentrations of 0.9 % and 20 μM, respectively) were dropped directly onto the agarose. When external electric field was applied during the observation, two platinum electrodes were dipped into the agarose and the whole specimen was covered by mineral oil to prevent heating. Standard power supply was used to keep the desired current flux of 15 mA (corresponds to 20 V) between the electrodes during the treatment.

Measurement of relative membrane potential

Membrane potential measurements using ^{3}H-TPP were performed as described by Vallejo and Serrano (1989). To 5 ml cells ($A_{600} = 20$) in growth medium, 1.2 μC of ^{3}H-TPP (specific activity 11 μC/μmol) was added and 0.5 ml withdrawn at the times indicated; radioactivity was measured by liquid scintillation counting.

Leakage experiments

AIB uptake and leakage were measured as in Komor *et al* (1979). Yeast cells were harvested during logarithmic growth, washed and resuspended in 25 mM sodium phosphate (pH 6.0) to a cell density of $A_{600} = 8.0$ OD and further incubated at 30°C with 1% glucose and 106 μM [^{14}C]AIB (2.8 mCi/mol). After 1.5–2 h, the AIB-loaded cells were collected, washed and resuspended in the same buffer containing only glucose. After 30 min equilibration, 20 μM FCCP and/or 0.1 or 0.5% SDS were added, and the disappearance of AIB radioactivity from the cells was followed in samples filtered and washed on glass fiber filters. Radioactivity was determined by liquid scintillation counting.

Supplementary data

Supplementary data are available at *The EMBO Journal* Online (http://www.embojournal.org).

Acknowledgements

The expert technical assistance of Ingrid Fuchs and Heidi Piberger is gratefully acknowledged. We thank Dr Jürgen Stolz (University of Regensburg) for provision of plasmids and helpful discussions. Financial support of DFG (Schwerpunkt 1108) and of Fonds der Chemischen Industrie is acknowledged. MO was also supported by LC545 and GA CR (204/06/0009) and JM by AS CR (AV0Z 50390512).

References

Aggeler R, Capaldi RA (1990) Yeast cytochrome *c* oxidase subunit VII is essential for assembly of an active enzyme. Cloning, sequencing, and characterization of the nuclear-encoded gene. *J Biol Chem* **265:** 16389–16393

Anderson RGW, Jacobson K (2002) A role of lipid shells in targeting proteins to caveolae, rafts, and other lipid domains. *Science* **296:** 1821–1825

Bagnat M, Keranen S, Shevchenko A, Simons K (2000) Lipid rafts function in biosynthetic delivery of proteins to the cell surface in yeast. *Proc Natl Acad Sci USA* **97:** 3254–3259

Brachmann CB, Davies A, Cost GJ, Caputo E, Li J, Hieter P, Boeke JD (1998) Designer deletion strains derived from *Saccharomyces cerevisiae* S288C: a useful set of strains and plasmids for PCR-mediated gene disruption and other applications. *Yeast* **14:** 115–132

Brown DA, London E (1998) Functions of lipid rafts in biological membranes. *Annu Rev Cell Dev Biol* **14:** 111–136

Bullock WO, Fernandez JM, Short JM (1987) XL1-Blue: a high efficiency plasmid transforming recA *Escherichia coli* strain with beta-galactosidase selection. *BioTechniques* **5:** 376–378

Dupre S, Haguenauer-Tsapis R (2003) Raft partitioning of the yeast uracil permease during trafficking along the endocytic pathway. *Traffic* **4:** 83–96

Edidin M (2003) The state of lipid rafts: from model membranes to cells. *Annu Rev Biophys Biomol Struct* **32:** 257–283

Gaigg B, Timischl B, Corbino L, Schneiter R (2005) Synthesis of sphingolipids with very long chain fatty acids but not ergosterol is required for routing of newly synthesized plasma membrane ATPase to the cell surface of yeast. *J Biol Chem* **280:** 22515–22522

Galbiati F, Razani B, Lisanti MP (2001) Emerging themes in lipid rafts and caveolae. *Cell* **106:** 403–411

Gietz RD, Sugino A (1988) New yeast–*Escherichia coli* shuttle vectors constructed with *in vitro* mutagenized yeast genes lacking six-base pair restriction sites. *Gene* **74:** 527–534

Grossmann G, Opekarova M, Novakova L, Stolz J, Tanner W (2006) Lipid raft-based membrane compartmentation of a plant transport protein expressed in *Saccharomyces cerevisiae*. *Eukaryot Cell* **5:** 945–953

Hearn JD, Lester RL, Dickson RC (2003) The uracil transporter Fur4p associates with lipid rafts. *J Biol Chem* **278:** 3679–3686

Heerklotz H (2002) Triton promotes domain formation in lipid raft mixtures. *Biophys J* **83:** 2693–2701

Herman P, Malinsky J, Plasek J, Vecer J (2004) Pseudo real-time method for monitoring of the limiting anisotropy in membranes. *J Fluoresc* **14:** 79–85

Kodama Y, Omura F, Takahashi K, Shirahige K, Ashikari T (2002) Genome-wide expression analysis of genes affected by amino acid sensor Ssy1p in *Saccharomyces cerevisiae*. *Curr Genet* **41:** 63–72

Komor E, Tanner W (1976) The determination of the membrane potential of *Chlorella vulgaris*. Evidence for electrogenic sugar transport. *Eur J Biochem* **70:** 197–204

Komor E, Weber H, Tanner W (1979) Greatly decreased susceptibility of nonmetabolizing cells towards detergents. *Proc Natl Acad Sci USA* **76:** 1814–1818

Kruijff B, Demel RA (1974) Polyene antibiotic–sterol interactions in membranes of *Acholeplasma laidlawii* cells and lecithin liposomes. 3. Molecular structure of the polyene antibiotic-cholesterol complexes. *Biochim Biophys Acta* **339:** 57–70

Kusumi A, Koyama-Honda I, Suzuki K (2004) Molecular dynamics and interactions for creation of stimulation –induced rafts. *Traffic* **5:** 213–230

Lagerholm BC, Weinreb GE, Jacobson K, Thompson NL (2005) Detecting microdomains in intact cell membranes. *Annu Rev Phys Chem* **56:** 309–336

Lauwers E, André B (2006) Association of yeast transporters with detergent-resistant membranes correlates with their cell-surface localization. *Traffic* **7:** 1045–1059

Lee MCS, Hamamoto S, Schekman R (2002) Ceramide biosynthesis is required for the formation of the oligomeric H^+-ATPase Pma1p in the yeast endoplasmic reticulum. *J Biol Chem* **277:** 22395–22401

Malewicz B, Borowski E (1979) Energy dependence and reversibility of membrane alterations induced by polyene macrolide antibiotics in *Chlorella vulgaris*. *Nature* **281:** 80–82

Malinska K, Malinsky J, Opekarova M, Tanner W (2003) Visualization of protein compartmentation within the plasma membrane of living yeast cells. *Mol Biol Cell* **14:** 4427–4436

Malinska K, Malinsky J, Opekarova M, Tanner W (2004) Distribution of Can1p into stable domains reflects lateral protein segregation within the plasma membrane of living *S. cerevisiae* cells. *J Cell Sci* **117:** 6031–6041

Munro S (2003) Lipid rafts: elusive or illusive? *Cell* **115:** 377–388

Norman AW, Demel RA, de Kruijff B, van Deenen LLM (1972) Studies on the biological properties of polyene antibiotics. Evidence for the direct interaction of filipin with cholesterol. *J Biol Chem* **247:** 1918–1929

Reifenberger E, Freidel K, Ciriacy M (1995) Identification of novel HXT genes in *Saccharomyces cerevisiae* reveals the impact of individual hexose transporters on glycolytic flux. *Mol Microbiol* **16:** 157–167

Robl I, Grassl R, Tanner W, Opekarova M (2000) Properties of a reconstituted eukaryotic hexose/proton symporter solubilized by structurally related non-ionic detergents: specific requirement of phosphatidylcholine for permease stability. *Biochim Biophys Acta* **1463:** 407–418

Roelants FM, Torrance PD, Bezman N, Thorner J (2002) Pkh1 and pkh2 differentially phosphorylate and activate ypk1 and ykr2 and define protein kinase modules required for maintenance of cell wall integrity. *Mol Biol Cell* **13:** 3005–3028

Sauer N, Caspari T, Klebl F, Tanner W (1990) Functional expression of the *Chlorella* hexose transporter in *Schizosaccharomyces pombe*. *Proc Natl Acad Sci USA* **87:** 7949–7952

Schäffer E, Thiele U (2004) Dynamic domain formation in membranes: thickness-modulation-induced phase separation. *Eur Phys J E* **14:** 169–175

Seron K, Blondel MO, Haguenauer-Tsapis R, Volland C (1999) Uracil-induced down-regulation of the yeast uracil permease. *J Bacteriol* **181:** 1793–1800

Simons K, Ikonen E (1997) Functional rafts in cell membranes. *Nature* **387:** 569–572

Steinmetz LM, Scharfe C, Deutschbauer AM, Mokranjac D, Herman ZS, Jones T, Chu AM, Giaever G, Prokisch H, Oefner PJ, Davis RW (2002) Systematic screen for human disease genes in yeast. *Nat Genet* **31:** 400–404

Takeda M, Chen WJ, Saltzgaber J, Douglas MG (1986) Nuclear genes encoding the yeast mitochondrial ATPase complex. Analysis of ATP1 coding the F1-ATPase alpha-subunit and its assembly. *J Biol Chem* **261:** 15126–15133

Umebayashi K, Nakano A (2003) Ergosterol is required for targeting of tryptophan permease to the yeast plasma membrane. *J Cell Biol* **161:** 1117–1131

Vallejo CG, Serrano R (1989) Physiology of mutants with reduced expression of plasma membrane H^+-ATPase. *Yeast* **4:** 307–319

Walther TC, Brickner JH, Aguilar PS, Bernales S, Pantoja C, Walter P (2006) Eisosomes mark static sites of endocytosis. *Nature* **439:** 998–1003

Young ME, Karpova TS, Brügger B, Moschenross DM, Wang GK, Schneiter R, Wieland FT, Cooper JA (2002) The Sur7p family defines novel cortical domains in *Saccharomyces cerevisiae*, affects sphingolipid metabolism, and is involved in sporulation. *Mol Cell Biol* **22:** 927–934

